Wave-Interactions in Quasi-Geostrophic Uniform Potential Vorticity Flow

WILLIAM BLUMEN

Department of Astro-Geophysics, University of Colorado, Boulder 80309

(Manuscript received 15 March 1982, in final form 29 June 1982)

ABSTRACT

A model of quasi-geostrophic uniform potential vorticity flow, previously examined by Blumen (1978a,b), is considered. The total depth-integrated energy and the available potential energy on level boundaries are conserved by the motion. Nonlinear interactions between three different scales of motion are examined. The linear system is first analyzed to determine the normal modes of the model. There are two sets of normal modes, corresponding to two different unstable growth rates. It is then shown that if normal mode initial conditions are specified for the nonlinear initial-value problem, the two conservation principles may be combined to yield a single constraint on the nonlinear interactions that occur between three scales of motion. The properties of normal mode initial conditions are also used to cast this constraint into a relatively simple form that is appropriate during the initial stages of the finite amplitude motion.

Numerical integrations of the basic set of equations reveal that the solutions are quite sensitive to the initial conditions. When normal mode initial conditions corresponding to the largest unstable growth rate are used, the simpler constraint continues to apply past the initial stages of growth. Analytical confirmation of this result is also provided. Nonlinear motions, associated with the other set of normal mode initial conditions, are also examined. The initial stages of the motion are similar to those above, but then the solutions tend to become aperiodic and the simpler form of the constraint on scale interactions does not apply. Extension of the range of integration over a broader range of initial conditions is suggested by these results.

1. Introduction

The effect of nonhomogeneous boundary conditions on the energy transfer properties of quasi-geostrophic uniform potential vorticity flow was examined by Blumen (1978a,b). The assumption of uniform potential vorticity implies that potential enstrophy conservation is identically satisfied: the conservation of available potential energy on level boundaries and conservation of depth-integrated total energy, provide the basic integral constraints on the flow.

A formal analogy was shown to exist between these latter constraints and the expressions for conservation of energy and potential enstrophy in a stratified fluid contained between two potential temperature surfaces. Energy exchanges between three different scales of motion were considered by Blumen (1978a, Section 3). However, in this model of uniform potential vorticity flow, the eigenfunctions are expressed in terms of both a symmetric and an antisymmetric function of height z, in order to satisfy the condition of potential temperature conservation at the top and bottom boundaries. In addition, the characteristic vertical scale, associated with energy exchanges, is not necessarily constant, but is a function of the motion. As a consequence, a scale-interaction theorem, similar to that derived by Fjørtoft (1953), could not be derived, except for the case when all the energy exchanges are restricted to relatively small-scale waves.

The purpose of the present paper is to develop a scale-interaction theorem, restricted to interactions between three scales of motion, that is not limited to a particular range of wavenumbers. The approach taken here is to define the initial state in terms of the normal modes of the system. Consequently, the results point up the role of initial conditions *and* the vertical structure of the waves on energy exchanges when nonzero temperature gradients exist on level boundaries. These aspects of wave energetics were not considered by either Fjørtoft, who considered barotropic flow, or by Charney (1971), who neglected temperature variations on the boundaries. However, the present results should only be viewed as a step in isolating fundamental processes that contribute to atmospheric and oceanic energy spectra, rather than as a low-order model analogue of real flows.

First, the basic nonlinear model equations are displayed in Section 2. Then normal modes of the complementary linear system are determined, and used in conjunction with conservative properties of the system to derive a scale-interaction theorem in Section 3. Extension to nonlinear wave-interactions is provided by a combined analytical and numerical treatment in Sections 4 and 5 and final remarks appear in Section 6. A solution of the nonlinear set of

0022-4928/82/112388-09$06.25

equations, satisfying normal mode initial conditions, is presented in Appendix C. The interested reader may follow the development without recourse to the appendices, which contain much of the mathematical detail.

2. Basic equations

The basic equations have been presented by Blumen (1978a,b, hereafter I and II). Briefly, the geostrophic streamfunction $\psi(x, y, z, t)$, which satisfies the condition of uniform potential vorticity, $\Delta\psi = 0$, in the interior flow may be represented by

$$\psi = \tfrac{1}{2}\sum_{-\infty}^{\infty}\sum_{-\infty}^{\infty}\{[A_{k,l}(t)\cosh\kappa_{k,l}z + B_{k,l}(t)\sinh\kappa_{k,l}z]e^{i(kx+ly)} + \text{c.c.}\}, \quad (1)$$

where $\kappa_{k,l}^2 = k^2 + l^2$ represents the sum of the squares of the (x, y) wavenumbers (k, l), the complex Fourier amplitudes $(A_{k,l}, B_{k,l})$ are functions of time t and (x, y, z) denote the usual Cartesian coordinates. In addition, all terms have been made nondimensional as in the notation of Pedlosky (1964).

The set of equations governing the amplitudes are determined by substitution of (1) into the appropriate condition at level boundaries, conservation of potential temperature $\theta = \psi_{z'}$

$$\psi_{zt} = \psi_y\psi_{zx} - \psi_x\psi_{zy}, \quad z = \pm\tfrac{1}{2}. \quad (2)$$

It has been shown in I (Section 3) that the conservation of the total depth-integrated energy $\mathcal{E}$ and the conservation of available potential energy on the boundaries $\mathcal{G}$ may be expressed as

$$\frac{d\mathcal{E}}{dt} = \frac{d}{dt}\sum_{-\infty}^{\infty}\sum_{-\infty}^{\infty}\kappa_{k,l}(a_{k,l}^2 + b_{k,l}^2)\sinh\kappa_{k,l}/2 \times \cosh\kappa_{k,l}/2 = 0, \quad (3)$$

$$\frac{d\mathcal{G}}{dt} = \frac{d}{dt}\sum_{-\infty}^{\infty}\sum_{-\infty}^{\infty}\kappa_{k,l}^2(a_{k,l}^2\sinh^2\kappa_{k,l}/2 + b_{k,l}^2\cosh^2\kappa_{k,l}/2) = 0, \quad (4)$$

where $a_{k,l}$ and $b_{k,l}$ are now real Fourier coefficients.

The approach to be taken here is to analyze the energy exchanges between three scales of motion denoted by $\kappa_i = (k_i^2 + l_i^2)^{1/2}$, where $i = 1, 2, 3$, and require that the vector wavenumbers κ_i sum to zero. The set of equations governing the real amplitudes (a_i, b_i), determined from (2), are the same at either boundary and given by

$$\frac{d}{dt}(\kappa_1\sinh\tfrac{1}{2}\kappa_1 a_1) + \Gamma[\cosh\tfrac{1}{2}\kappa_2\cosh\tfrac{1}{2}\kappa_3(m_{S3} - m_{S2})a_2a_3 - \sinh\tfrac{1}{2}\kappa_2\sinh\tfrac{1}{2}\kappa_3(m_{A3} - m_{A2})b_2b_3] = 0, \quad (5)$$

$$\frac{d}{dt}(\kappa_1\cosh\tfrac{1}{2}\kappa_1 b_1) - \Gamma[\cosh\tfrac{1}{2}\kappa_2\sinh\tfrac{1}{2}\kappa_3(m_{A3} - m_{S2})a_2b_3 + \sinh\tfrac{1}{2}\kappa_2\cosh\tfrac{1}{2}\kappa_3(m_{S3} - m_{A2})a_3b_2] = 0, \quad (6)$$

$$\frac{d}{dt}(\kappa_2\sinh\tfrac{1}{2}\kappa_2 a_2) - \Gamma[\cosh\tfrac{1}{2}\kappa_1\cosh\tfrac{1}{2}\kappa_3(m_{S3} - m_{S1})a_1a_3 - \sinh\tfrac{1}{2}\kappa_1\sinh\tfrac{1}{2}\kappa_3(m_{A3} - m_{A1})b_1b_3] = 0, \quad (7)$$

$$\frac{d}{dt}(\kappa_2\cosh\tfrac{1}{2}\kappa_2 b_2) + \Gamma[\cosh\tfrac{1}{2}\kappa_1\sinh\tfrac{1}{2}\kappa_3(m_{A3} - m_{S1})a_1b_3 + \sinh\tfrac{1}{2}\kappa_1\cosh\tfrac{1}{2}\kappa_3(m_{S3} - m_{A1})a_3b_1] = 0, \quad (8)$$

$$\frac{d}{dt}(\kappa_3\sinh\tfrac{1}{2}\kappa_3 a_3) + \Gamma[\cosh\tfrac{1}{2}\kappa_1\cosh\tfrac{1}{2}\kappa_2(m_{S2} - m_{S1})a_1a_2 - \sinh\tfrac{1}{2}\kappa_1\sinh\tfrac{1}{2}\kappa_2(m_{A2} - m_{A1})b_1b_2] = 0, \quad (9)$$

$$\frac{d}{dt}(\kappa_3\cosh\tfrac{1}{2}\kappa_3 b_3) - \Gamma[\cosh\tfrac{1}{2}\kappa_1\sinh\tfrac{1}{2}\kappa_2(m_{A2} - m_{S1})a_1b_2 + \sinh\tfrac{1}{2}\kappa_1\cosh\tfrac{1}{2}\kappa_2(m_{S2} - m_{A1})a_2b_1] = 0, \quad (10)$$

where $\Gamma = (l_2k_3 - l_3k_2)/2$[1] and

$$m_{Si} = \kappa_i\tanh\kappa_i/2, \quad m_{Ai} = \kappa_i\coth\kappa_i/2. \quad (11)$$

It may be verified that this truncated system, (5)–(10), satisfies the constraints of total energy conservation and conservation of available potential energy on level boundaries, given by (3) and (4).

3. Normal modes

a. Solutions

The normal modes are obtained from the linear system, determined by linearizing the equations around the state (a_1, b_1), equal to a constant with $a_2 = b_2 = a_3 = b_3 = 0$. The perturbation amplitudes (a_3, b_3) may then be eliminated between (7)–(10) to yield the second-order differential equations

$$\ddot{a}_2 + f_1a_2 = g_1b_2, \quad (12a)$$

$$\ddot{b}_2 + f_2b_2 = -g_2a_2, \quad (12b)$$

[1] In II (Section 2), doubly periodic wave solutions in a channel were employed, which reduced Γ by an additional factor of one-half; otherwise the basic equations are identical.

where

$$f_1 = \Gamma^2\left[\left(\frac{m_{S3}-m_{S1}}{m_{S3}}\right)\left(\frac{m_{S2}-m_{S1}}{m_{S2}}\right)\cosh^{2}\tfrac{1}{2}\kappa_1 a_1^2 + \left(\frac{m_{A3}-m_{A1}}{m_{A3}}\right)\left(\frac{m_{S2}-m_{A1}}{m_{S2}}\right)\sinh^{2}\tfrac{1}{2}\kappa_1 b_1^2\right], \quad (13a)$$

$$f_2 = \Gamma^2\left[\left(\frac{m_{A3}-m_{S1}}{m_{A3}}\right)\left(\frac{m_{A2}-m_{S1}}{m_{A2}}\right)\cosh^{2}\tfrac{1}{2}\kappa_1 a_1^2 + \left(\frac{m_{S3}-m_{A1}}{m_{S3}}\right)\left(\frac{m_{A2}-m_{A1}}{m_{A2}}\right)\sinh^{2}\tfrac{1}{2}\kappa_1 b_1^2\right], \quad (13b)$$

$$g_1 = (\Gamma^2/\kappa_2)\left[\left(\frac{m_{S3}-m_{S1}}{m_{S3}}\right)(m_{A2}-m_{A1}) - \left(\frac{m_{A3}-m_{A1}}{m_{A3}}\right)(m_{A2}-m_{S1})\right]\sinh\tfrac{1}{2}\kappa_1 \cosh\tfrac{1}{2}\kappa_1 a_1 b_1, \quad (13c)$$

$$g_2 = (\Gamma^2/\kappa_2)\left[\left(\frac{m_{A3}-m_{S1}}{m_{A3}}\right)(m_{S2}-m_{A1}) - \left(\frac{m_{S3}-m_{A1}}{m_{S3}}\right)(m_{S2}-m_{S1})\right]\sinh\tfrac{1}{2}\kappa_1 \cosh\tfrac{1}{2}\kappa_1 a_1 b_1, \quad (13d)$$

Γ is defined below (10) and (m_{Si}, m_{Ai}) are given by (11).

This set (12a,b) has the same form as the equations of motion of a linear system of coupled oscillators, e.g., Morse and Ingard (1968). The normal modes of this system, derived in Appendix A, are solutions of

$$\ddot{X}_1 - \sigma_-^2 X_1 = 0, \quad (14a)$$

$$\ddot{X}_2 - \sigma_+^2 X_2 = 0, \quad (14b)$$

where the relative growth rates are given by the positive roots of

$$\sigma_\pm^2 = -\tfrac{1}{2}(f_1 + f_2) \pm \tfrac{1}{2}[(f_1 + f_2)^2 - 4(f_1 f_2 + g_1 g_2)]^{1/2}, \quad (15)$$

and (f_i, g_i) are given by (13). The normal modes are defined as

$$X_1 = a_2 - \Gamma_1 b_2 = C_1 e^{\sigma_- t} + D_1 e^{-\sigma_- t}, \quad (16a)$$

$$X_2 = b_2 - \Gamma_2 a_2 = C_2 e^{\sigma_+ t} + D_2 e^{-\sigma_+ t}, \quad (16b)$$

where C_j and D_j $(j = 1, 2)$ are constants and

$$\Gamma_1 = \frac{g_1}{\sigma_+^2 + f_1} = -\frac{\sigma_+^2 + f_2}{g_2}, \quad (17a)$$

$$\Gamma_2 = -\frac{g_2}{\sigma_-^2 + f_2} = \frac{\sigma_-^2 + f_1}{g_1}. \quad (17b)$$

b. Conservation property

It is apparent from (14a, b) that the energy associated with the individual normal modes is conserved; energy is not exchanged between them. It is possible to establish a conservative property of this linear system, based on the independence of normal mode solutions. The proof appears in Appendix B. The result is

$$\frac{1}{2}\frac{d}{dt}\{(\lambda_2 - \lambda_1)M_2 + (\lambda_3 - \lambda_1)M_3\} = 0, \quad (18)$$

where

$$M_i = (a_i^2 + b_i^2)\kappa_i \sinh\tfrac{1}{2}\kappa_i \cosh\tfrac{1}{2}\kappa_i, \quad (19)$$

$$\lambda_i = \frac{m_{Si}a_i^2 + m_{Ai}b_i^2}{a_i^2 + b_i^2}, \quad (20)$$

and (m_{Si}, m_{Ai}) are defined by (11).

The conservation property expressed by (18) holds for modes associated with *either* growth rate σ_+ *or* growth rate σ_-, but not their sum. In view of the time dependence of the amplitude, expressed by (16a) or (16b), (18) reduces to

$$(\lambda_2 - \lambda_1)M_2 + (\lambda_3 - \lambda_1)M_3 = 0. \quad (21)$$

Numerical evaluation of $\sigma_\pm$ and the corresponding amplitudes, over a wide range of parameters, has been carried out to verify (21). Use will be made of this result in the following section.

4. Scale-interaction theorem

The two conservation principles satisfied by the *nonlinear* system, (5)–(10), are expressed by (3) and (4). These are conservation of total depth-integrated energy

$$M_1 + M_2 + M_3 = \mathcal{E}(0), \quad (22)$$

and conservation of available potential energy on level boundaries

$$\lambda_1 M_1 + \lambda_2 M_2 + \lambda_3 M_3 = \mathcal{G}(0), \quad (23)$$

where M_i and λ_i are defined by (19) and (20) and $\mathcal{E}(0)$ and $\mathcal{G}(0)$ denote initial values. In addition, the ratio of the energies,

$$\frac{\lambda_1 M_1 + \lambda_2 M_2 + \lambda_3 M_3}{M_1 + M_2 + M_3} = \frac{\mathcal{G}(0)}{\mathcal{E}(0)}, \quad (24)$$

is conserved since $\mathcal{G}$ and $\mathcal{E}$ are individually conserved.

As pointed out in I (Section 3), m_{Si} and m_{Ai} are characteristic vertical scales associated with the symmetric (S) and antisymmetric (A) vertical structures of the eigenfunctions. The quantity λ_i may also be interpreted as the wavenumber of the centroid of (a_i^2, b_i^2) associated respectively with "vertical wavenumbers" (m_{Si}, m_{Ai}). Since λ_i is function of the motion, expressed by the dependence on (a_i^2, b_i^2), it is not obvious how (22) and (23) provide constraints on

scale interactions; the proper choice of initial conditions appears to be crucial.

First (22) and (23) are combined to yield

$$[\lambda_1 - \lambda_1(0)]M_1 + [\lambda_2 - \lambda_1(0)]M_2 + [\lambda_3 - \lambda_1(0)]M_3 = [(\lambda_2 - \lambda_1)M_2 + (\lambda_3 - \lambda_1)M_3]_{t=0}, \quad (25)$$

where $\lambda_1(0)$ denotes the value at $t = 0$. It will be assumed hereafter that initially ($t = 0$), $\lambda_2 < \lambda_1 < \lambda_3$, otherwise the value of the right-hand side may be specified arbitrarily. If a linear normal mode solution is used for the initial state, then (21) may be used to reduce (25) to

$$[\lambda_1 - \lambda_1(0)]M_1 + [\lambda_2 - \lambda_1(0)]M_2 + [\lambda_3 - \lambda_1(0)]M_3 = 0. \quad (26)$$

This expression (26) constitutes the nonlinear scale-interaction theorem for quasi-geostrophic uniform potential vorticity flow initiated by a normal mode solution of the corresponding linear system. In addition, (24) may be reduced to

$$\lambda_1(0) = \mathcal{G}(0)/\mathcal{E}(0) \quad (27)$$

by the introduction of (26).

When the motions are small enough to be governed by the linearized equations, (26) reduces to (21). In this latter case, similar to Fjørtoft's (1953) result, energy flows from the wave with the intermediate vertical scale λ_1, to waves characterized by both longer and shorter vertical scales. When κ_i is relatively large, (26) also reduces to the form of (21) with $\lambda_i \approx \kappa_i$. However, energy may flow from or to the intermediate wave in this latter case which is not restricted by either linearization or by the use of normal mode initial conditions.

The constraint provided by (26) is weaker than that provided by these limiting cases, because the inequalities $\lambda_2 < \lambda_1 < \lambda_3$ need not be preserved by the motion. However, a unidirectional energy cascade to scales of motion λ_i that are all either larger or smaller than the initial scale $\lambda_1(0)$ is prevented by (26).

The analysis may be carried further in order to simplify (26). First, $\lambda_1(t)$ is expanded in the form

$$\lambda_1(t) = \lambda_1(0) + (d\lambda_1/dt)_{t=0}t + \tfrac{1}{2}(d^2\lambda_1/dt^2)_{t=0}t^2 + \cdots. \quad (28)$$

An expression for $d\lambda_1/dt$ may be obtained by noting that

$$M_1^2 d\lambda_1/dt = M_1 d(\lambda_1 M_1)/dt - \lambda_1 M_1 dM_1/dt, \quad (29)$$

where M_1 and λ_1 are defined by (19) and (20). The right-hand side (rhs) of (29) may be evaluated from (5) and (6) to obtain

$$\begin{aligned} M_1^2 d\lambda_1/dt = {} & \Gamma\kappa_1 \sinh\tfrac{1}{2}\kappa_1 \cosh\tfrac{1}{2}\kappa_1(m_{A1} - m_{S1})a_1b_1 \\ & \times \{\cosh\tfrac{1}{2}\kappa_1 \cosh\tfrac{1}{2}\kappa_2 \cosh\tfrac{1}{2}\kappa_3(m_{S3} - m_{S2})a_2a_3b_1 \\ & - \cosh\tfrac{1}{2}\kappa_1 \sinh\tfrac{1}{2}\kappa_2 \sinh\tfrac{1}{2}\kappa_3(m_{A3} - m_{A2})b_1b_2b_3 \\ & + \sinh\tfrac{1}{2}\kappa_1 \cosh\tfrac{1}{2}\kappa_2 \sinh\tfrac{1}{2}\kappa_3(m_{A3} - m_{S2})a_1a_2b_3 \\ & + \sinh\tfrac{1}{2}\kappa_1 \sinh\tfrac{1}{2}\kappa_2 \cosh\tfrac{1}{2}\kappa_3(m_{S3} - m_{A2})a_1a_3b_2\}. \end{aligned} \quad (30)$$

The expression in braces on the rhs of (30) vanishes when it is evaluated by a normal mode initial state, as shown in Appendix B. Then the first non-zero contribution to the term $[\lambda_1 - \lambda_1(0)]$ in (26) would be associated with a term of $O(t^2)$. At least to this order of the approximation,

$$\lambda_1(t) \approx \lambda_1(0), \quad (31)$$

$$(\lambda_2 - \lambda_1)M_2 + (\lambda_3 - \lambda_1)M_3 \approx 0. \quad (32)$$

This result, (31) and (32), represents an extension of (21) to encompass finite-amplitude wave-interactions during the early stages of the motion, when a normal mode initial condition is specified. Numerical integrations will now be used to illustrate various results that have been established analytically, and to determine the extent to which (31) and (32) constrain finite amplitude motions.

5. Numerical results

For numerical purposes, the wavenumbers are expressed as

$$\left.\begin{aligned} k_1 &= r_1 \cos\theta_1, \quad l_1 = r_1 \sin\theta_1 \\ k_2 &= r_2 \cos\theta_2, \quad l_2 = r_2 \sin\theta_2 \end{aligned}\right\}, \quad (33)$$

where

$$\kappa_1 = r_1, \quad \kappa_2 = r_2,$$

$$\kappa_3 = (r_1^2 + r_2^2 + 2r_1r_2 \cos\theta)^{1/2}, \quad (34)$$

and $\theta = \theta_2 - \theta_1$ denotes the angle between the vector wavenumbers $\mathbf{r}_1$ and $\mathbf{r}_2$. The unstable growth rates $\sigma_\pm$, given by (15), were determined over the range $0 \leqslant \theta \leqslant \pi$, for values $0.5 \leqslant r_1 \leqslant 4.0$. A representative distribution of amplitudes was chosen in the range $0.1 \leqslant (a_1, b_1) \leqslant 1.0$. The results, which need not be displayed here, show that:

1) The maximum growth rates tend to occur in the range $\pi/3 \leqslant \theta \leqslant \pi/2$.

2) When $r_1 \leqslant 2$, $\sigma_-/\sigma_+ \approx 10^{-1}$.

3) The range of $\sigma_- > 0$ is much less than the range of $\sigma_+ > 0$, which could be anticipated by inspection of (15).

It is impractical to carry out numerical integrations of (5)–(10) over the whole range of parameter values used for the growth rate calculations. For present

purposes, the range of θ was restricted to $\pi/3 \leqslant \theta \leqslant \pi/2$ with (a_1, b_1) both varied in $0.1 \leqslant (a_1, b_1) \leqslant 1.0$. The wavenumbers $\kappa_1 \geqslant 1$ and $\kappa_2 \leqslant 1$ were specified and κ_3 was determined by (34). The amplitude a_2 was specified initially and the remaining amplitudes (a_3, b_2, b_3) calculated from the linear normal mode results. The case presented here is representative of all the integrations that have been carried out. The following parameter values apply:

$$r_1 = 1.5, \quad r_2 = 1.0, \quad r_3 = (3.25)^{1/2},$$
$$\theta = \pi/2,$$
$$a_1 = 0.5, \quad b_1 = -1.0,$$
$$\sigma_+ = 2.21372 \times 10^{-1},$$
$$\sigma_- = 3.30820 \times 10^{-2},$$
$$0.1 \leqslant a_2 \leqslant 1.0, \quad \Delta a_2 = 0.1,$$
$$0 \leqslant t \leqslant 100, \quad \Delta t = 1,$$
$$100 \leqslant t \leqslant 200, \quad \Delta t = 2.$$

The cases associated with $|a_1| = |b_1| = 1$ are not displayed because $\sigma_-^2 < 0$.

The numerical integrations were monitored by evaluating (26) at each time step. Virtually no loss of accuracy occurred over the time period examined. Some characteristics of the motion determined from the normal mode initial state associated with σ_+ are shown in Fig. 1. For this case, as well as the other cases not shown, the characteristics of the motion over the whole range of integration employed are constrained by

$$\lambda_i(t) = \lambda_i(0), \quad i = 1, 2, 3 \tag{35}$$

and

$$(\lambda_2 - \lambda_1)M_2 + (\lambda_3 - \lambda_1)M_3 = 0, \tag{36}$$

when the normal modes corresponding to σ_+, defined by (15), are used to provide the initial state. Moreover, the constant values of λ_i $(i = 1, 2, 3)$:

$$\left.\begin{aligned}\lambda_1 &= 2.07987\\ \lambda_2 &= 1.99098\\ \lambda_3 &= 2.43076\end{aligned}\right\} \tag{37}$$

are the same for all values of a_2 examined, $0.1 \leqslant a_2 \leqslant 1.0$.

Analytic solutions, derived in Appendix C, may be represented as

$$b_1 = A_1(r_i, \theta)\mathcal{E}^{1/2} \tanh[B_1(r_i, \theta)\mathcal{E}^{1/2}(t_0 - t)], \tag{38}$$

$$a_2 = A_2(r_i, \theta)\mathcal{E}^{1/2} \operatorname{sech}[B_2(r_i, \theta)\mathcal{E}^{1/2}(t_0 - t)], \tag{39}$$

where $\mathcal{E} = \mathcal{E}(0)$, defined by (22), represents the initial value of the depth-integrated energy and

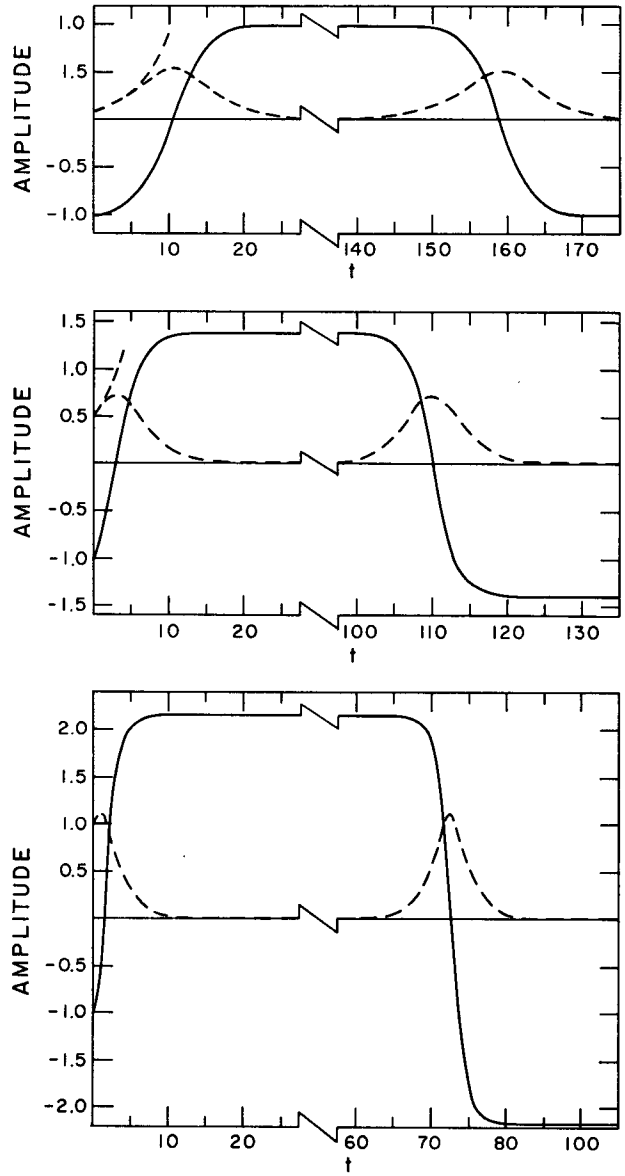

FIG. 1. Amplitudes b_1 (solid) and a_2 (dashed) as functions of time t, determined from the normal mode initial state associated with growth rate σ_+. The three figures correspond to the initial amplitudes $a_2 = 0.1$, 0.5 and 1.0. The other parameter values are provided in the text. The short dashed segment in the top two figures shows the linear unstable growth represented by $a_2(t) = a_2(0) \exp\sigma_+ t$.

$$t_0 = \frac{\tanh^{-1}\{b_1(0)[A_1(r_i, \theta)\mathcal{E}^{1/2}]^{-1}\}}{B_1(r_i, \theta)\mathcal{E}^{1/2}}. \tag{40}$$

The coefficients $A_{1,2}$ and $B_{1,2}$ are constants, evaluated from the values presented above. These solutions show that the asymptotic level of b_1 (and a_1) increases in proportion to $\mathcal{E}^{1/2}$ and that t_0 decreases as $\mathcal{E}^{1/2}$ increases, approaching $t_0 \propto \mathcal{E}^{-1}$ for large values of $\mathcal{E}$. Both properties of the solution are confirmed by

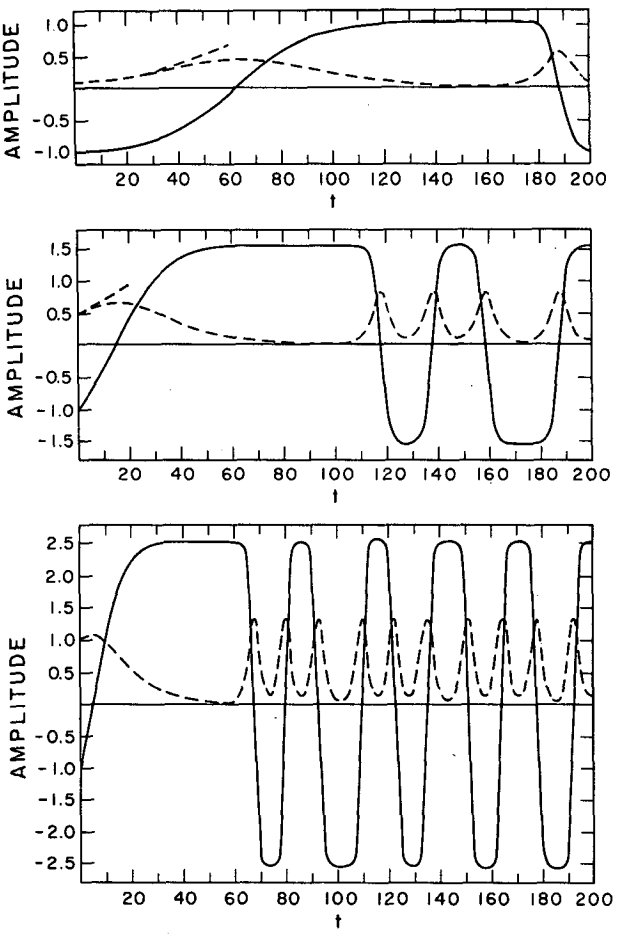

FIG. 2. As in Fig. 1, except growth rate σ_- applies.

the numerical results shown in Fig. 1. The analytic solutions, however, do not describe the solution over the complete range of t exhibited in Fig. 1: the pattern appears to be cyclic rather than remaining asymptotically steady as represented by (38) and (39).

TABLE 1. Minima of a_2: times and periods.

T^*	ΔT^{**}
56.625	
73.75	17.125
86.00	12.25
101.00	15.00
115.75	14.75
128.25	12.50
143.00	14.75
157.50	14.50
170.25	12.75
184.75	14.50
198.75	14.00

* T is time of minimum a_2.
** ΔT is the time between successive minima.

Nonetheless, the numerical solutions continue to satisfy (35) and (36) throughout the whole range of integration.

The numerical solutions for a_2 and b_1, corresponding to the normal mode initial state associated with σ_-, are presented in Fig. 2. The early evolution of the finite amplitude motion is clearly represented by the solutions given by (38), (39) and (40). Consequently, the motion satisfies the constraints provided by (35) and (36) with

$$\left.\begin{aligned}\lambda_1 &= 2.07987\\ \lambda_2 &= 2.07457\\ \lambda_3 &= 2.50457\end{aligned}\right\}. \tag{41}$$

After a period of time, determined by the initial amplitudes, the flow adopts a relatively aperiodic behavior. The aperiodicity was confirmed by rerunning the calculations for $a_2(0) = 1.0$ with step sizes $\Delta t = 0.125$ in $0 \leqslant t \leqslant 100$ and $\Delta t = 0.25$ in $100 \leqslant t \leqslant 200$. Periods, corresponding to the minima of a_2, are displayed in Table 1. However, the aperiodicity

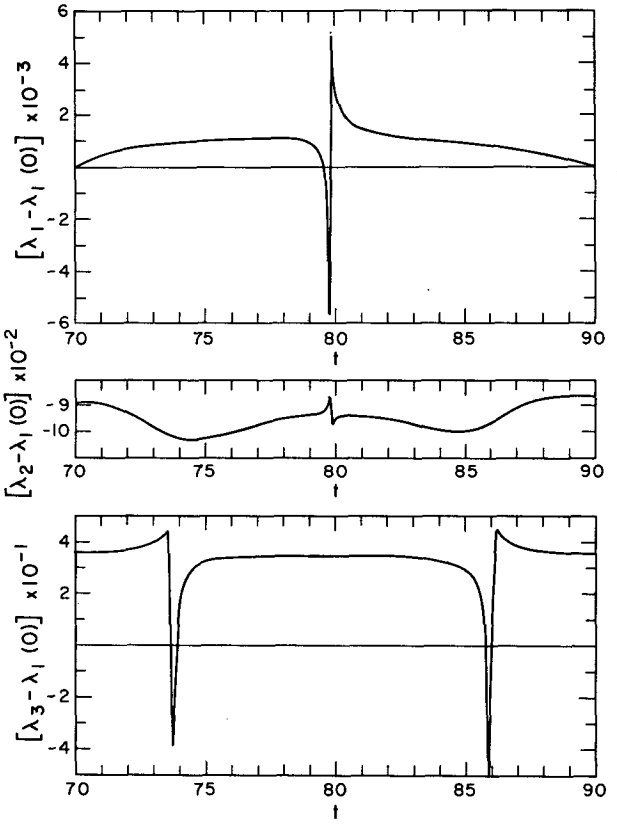

FIG. 3. Variations of $\lambda_i(t) - \lambda_1(0)$, defined by (20), in the range $70 \leqslant t \leqslant 90$, which are typical of variations that occur throughout the range $56.625 \leqslant t \leqslant 200$. The initial amplitude is $a_2 = 1$ and the normal mode initial state corresponds to growth rate σ_-. The other parameter values are as in Fig. 2.

has not been confirmed by carrying out integrations over a much longer time period.

At the onset of the change in the character of the solution and thereafter ($56.625 \leqslant t \leqslant 200$), the appropriate constraint on the motion reverts to (26) from (35) and (36). This circumstance arises in conjunction with changes in the λ_i ($i = 1, 2, 3$), shown in Fig. 3. Both relatively long and relatively short period fluctuations occur. The corresponding changes in the depth-integrated and available potential energies are displayed in Fig. 4. Comparison of Figs. 3 and 4 reveals that the most rapid change in λ_3, for example, occurs when the energies associated with (a_1, b_1) reach a maximum, and the remaining energies attain minimum values. The opposite situation is associated with the rapid changes in λ_1 and λ_2. In effect, the wavenumbers λ_i of the centroids of (a_i^2, b_i^2) must change abruptly in order to satisfy the constraint on the motion (26) whenever extremums in the energies are attained.

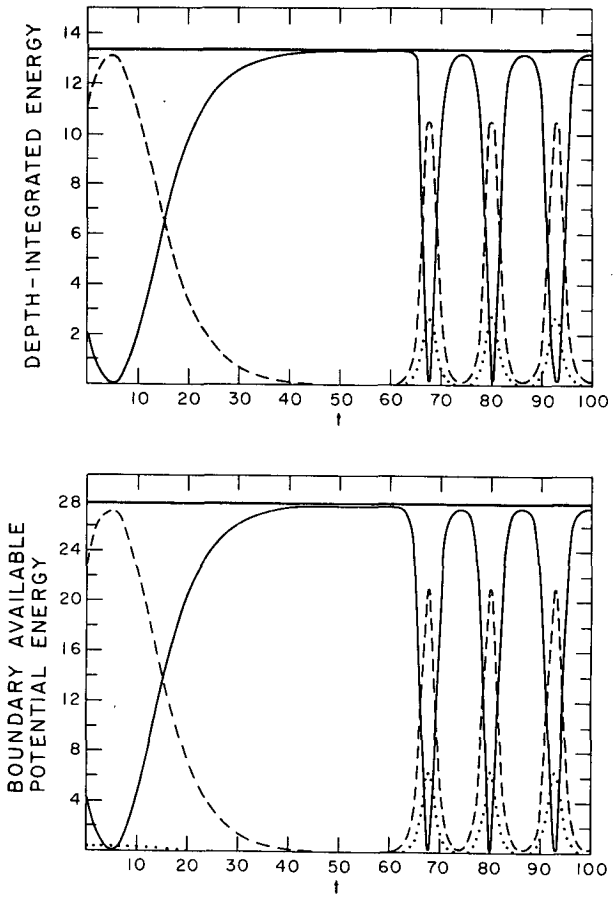

FIG. 4. Depth-integrated energy M_i and available potential energy on the boundary $\lambda_i M_i$, defined by (19) and (20), as functions of time t. The parameter values are as in Fig. 3. The solid, dashed and dotted lines correspond to $i = 1$, 2, and 3.

6. Remarks

The principal result is the establishment of a scale-interaction theorem for quasi-geostrophic uniform potential vorticity flow, expressed by (26). The theorem applies to a truncated system, consisting of three wavenumbers κ_i ($i = 1, 2, 3$), that satisfies the same quadratic constraints as the infinite-dimensional system, namely, the total depth-integrated energy and the available potential energy on the boundaries. Associated with each wavenumber κ_i are two waves: one with a symmetric vertical structure and one with an antisymmetric vertical structure. The presence of both are required to satisfy the boundary conditions, expressed by (2).

It has been shown that linear normal modes of this system can be derived and expressed in terms of linear combinations of the amplitudes (a_i, b_i), associated respectively with the symmetric and antisymmetric vertical structures. The theorem applies to nonlinear wave-interactions that are associated with normal mode initial conditions. There are two cases to consider because there are two sets of normal modes corresponding to different unstable growth rates of the linear system. Solutions, corresponding to each type of normal mode initial condition, are determined by numerical integrations and displayed in Figs. 1 and 2. The numerical results, shown in Figs. 3 and 4, also point up how the initial conditions affect the nonlinear transfer of energy between the waves. However, these results are only based on a relatively small subset of solutions in parameter space and the integrations have been terminated at $t = 200$. Characteristics of the solutions over longer time periods will be considered in future work. Yet the present results do complement the Fjørtoft scale-interaction theorem which applies to motions constrained by quasi-geostrophic energy and enstrophy or potential enstrophy conservation. Complementary application to studies of nonlinear wave-interactions between large-scale atmospheric and oceanic motions could be anticipated.

Acknowledgments. Financial support has been provided by the National Science Foundation under Grant No. ATM-8020138. Appreciation is also expressed to Kelly Kanizay for computational assistance, and to Julianna Chow of the National Center for Atmospheric Research for providing the numerical algorithm to solve system (5)–(10).

APPENDIX A

Normal Modes

The normal mode solutions (X_1, X_2), defined by (16a, b) are derived from the linear system of equations (12a, b). The amplitudes (a_2, b_2) that satisfy (12a, b) may be expressed as

$$\left.\begin{aligned} a_2 &= a_{12}e^{\sigma_+ t} + a_{22}e^{-\sigma_+ t} + a_{32}e^{\sigma_- t} + a_{42}e^{-\sigma_- t} \\ b_2 &= b_{12}e^{\sigma_+ t} + b_{22}e^{-\sigma_+ t} + b_{32}e^{\sigma_- t} + b_{42}e^{-\sigma_- t} \end{aligned}\right\}, \quad \text{(A1)}$$

where $\sigma_\pm$ are given by (15) and the coefficients in (A1) are all constants. Relationships between those coefficients may be obtained from (12a, b). They are given by

$$\left.\begin{aligned} a_{j,2} &= \Gamma_1 b_{j,2}\,, \quad j = 1, 2 \\ b_{k,2} &= \Gamma_2 a_{k,2}\,, \quad k = 3, 4 \end{aligned}\right\}, \quad \text{(A2)}$$

where (Γ_1, Γ_2) are defined by (17a, b). Introduction of (A2) into (A1) yields

$$\left.\begin{aligned} X_1 &\equiv a_2 - \Gamma_1 b_2 = C_1 e^{\sigma_- t} + D_1 e^{-\sigma_- t} \\ X_2 &\equiv b_2 - \Gamma_2 a_2 = C_2 e^{\sigma_+ t} + D_2 e^{-\sigma_+ t} \end{aligned}\right\}, \quad \text{(A3)}$$

where C_j and D_j $(j = 1, 2)$ are constants. Alternatively, the amplitudes (a_2, b_2) may be expressed as

$$\left.\begin{aligned} a_2 &= (X_1 + \Gamma_1 X_2)(1 - \Gamma_1\Gamma_2)^{-1} \\ b_2 &= (X_2 + \Gamma_2 X_1)(1 - \Gamma_1\Gamma_2)^{-1} \end{aligned}\right\}, \quad \text{(A4)}$$

where $1 - \Gamma_1\Gamma_2 \neq 0$ when $\sigma_+ \neq \sigma_-$. Substitution of (A4) into (12a, b) yields two simultaneous equations for (X_1, X_2), which may be reduced to (14a, b). The amplitudes (X_1, X_2), represented as linear combinations of (a_2, b_2), are called the normal modes of the system.

APPENDIX B

Conservation Principle for the Linear System

The linear system of equations consists of (7)–(10) with (a_1, b_1) as constants. A conservation principle may be derived from this system by showing that the rhs of the expression presented in (18) vanishes:

$$\begin{aligned} &\cosh\tfrac{1}{2}\kappa_1 \cosh\tfrac{1}{2}\kappa_2 \cosh\tfrac{1}{2}\kappa_3(m_{S3} - m_{S2})(\lambda_1 - m_{S1}) \\ &\times a_1a_2a_3 - \cosh\tfrac{1}{2}\kappa_1 \sinh\tfrac{1}{2}\kappa_2 \sinh\tfrac{1}{2}\kappa_3(m_{A3} - m_{A2}) \\ &\times (\lambda_1 - m_{S1})a_1b_2b_3 + \sinh\tfrac{1}{2}\kappa_1 \cosh\tfrac{1}{2}\kappa_2 \sinh\tfrac{1}{2}\kappa_3 \\ &\times (m_{S2} - m_{A3})(\lambda_1 - m_{A1})a_2b_1b_3 + \sinh\tfrac{1}{2}\kappa_1 \sinh\tfrac{1}{2}\kappa_2 \\ &\times \cosh\tfrac{1}{2}\kappa_3(m_{A2} - m_{S3})(\lambda_1 - m_{A1})a_3b_1b_2 = 0, \end{aligned} \quad \text{(B1)}$$

where (m_{Si}, m_{Ai}) are defined by (11) and λ_1 is defined by (20). Introduction of λ_1 into (B1) yields

$$\begin{aligned} &\cosh\tfrac{1}{2}\kappa_1 \cosh\tfrac{1}{2}\kappa_2 \cosh\tfrac{1}{2}\kappa_3(m_{S3} - m_{S2})a_2a_3b_1 \\ &- \cosh\tfrac{1}{2}\kappa_1 \sinh\tfrac{1}{2}\kappa_2 \sinh\tfrac{1}{2}\kappa_3(m_{A3} - m_{A2})b_1b_2b_3 \\ &+ \sinh\tfrac{1}{2}\kappa_1 \cosh\tfrac{1}{2}\kappa_2 \sinh\tfrac{1}{2}\kappa_3(m_{A3} - m_{S2})a_1a_2b_3 \\ &- \sinh\tfrac{1}{2}\kappa_1 \sinh\tfrac{1}{2}\kappa_2 \cosh\tfrac{1}{2}\kappa_3(m_{A2} - m_{S3})a_1a_3b_2 = 0. \end{aligned} \quad \text{(B2)}$$

A considerable amount of algebra is needed to establish (B2); only an outline will be presented.

The amplitudes (a_3, b_3) may be eliminated from (B2) by means of (9) and (10), using the solutions associated with either growth rate σ_+ or σ_-. After rearrangement, (B2) may be expressed as

$$g_2a_2^2 + (f_2 - f_1)a_2b_2 + g_1b_2^2 = 0, \quad \text{(B3)}$$

where (f_i, g_i) are defined by (13a, b, c, d). The solution of (B3) is

$$\begin{aligned} a_2 &= \frac{1}{2g_2}\{(f_1 - f_2) \pm [(f_1 - f_2)^2 - 4g_1g_2]^{1/2}\}b_2 \\ &= \frac{1}{2g_2}\{(f_1 - f_2) \\ &\qquad \pm [(f_1 + f_2)^2 - 4(f_1f_2 + g_1g_2)]^{1/2}\}b_2\,. \end{aligned} \quad \text{(B4)}$$

The negative root of (B4) leads to

$$a_2 = -\frac{(\sigma_+^2 + f_2)}{g_2}b_2 = \Gamma_1 b_2\,; \quad \text{(B5)}$$

the positive root yields

$$b_2 = -\frac{g_2}{\sigma_-^2 + f_2}a_2 = \Gamma_2 a_2\,. \quad \text{(B6)}$$

These expressions (B5, B6) are the same relationships established between the coefficients of the solutions associated with growth rates σ_+ and σ_- in (A2). These are the normal mode solutions. Then the conservation principle (18) is satisfied when a normal mode solution is used to evaluate (B1).

APPENDIX C

A Nonlinear Solution

It is possible to derive a nonlinear analytical solution by making use of the constraints provided by (35) and (36). The constancy of λ_i $(i = 1, 2, 3)$, expressed by (35), represents three relationships between a_i and b_i. As a consequence (36) may be reduced to a relationship between two amplitudes, say, a_2 and b_3. Then (6) may be expressed as

$$\begin{aligned} \frac{db_1}{dt} &= \left(\frac{\Gamma}{\beta\kappa_1 \cosh\tfrac{1}{2}\kappa_1}\right) \\ &\times \left\{\cosh\tfrac{1}{2}\kappa_2 \sinh\tfrac{1}{2}\kappa_3(m_{A3} - m_{S2})\left(\frac{\lambda_3 - m_{S3}}{m_{A2} - \lambda_2}\right)^{1/2}\right. \\ &+ \sinh\tfrac{1}{2}\kappa_2 \cosh\tfrac{1}{2}\kappa_3(m_{S3} - m_{A2}) \\ &\left.\times \left[\frac{m_{A3} - \lambda_3}{m_{A2} - \lambda_2}\frac{\lambda_2 - m_{S2}}{m_{A2} - \lambda_2}\right]^{1/2}\right\}a_2^2, \end{aligned} \quad \text{(C1)}$$

where

$$\beta^2 = \left(\frac{\lambda_3 - \lambda_1}{\lambda_1 - \lambda_2}\right)\left(\frac{m_{A3} - m_{S3}}{m_{A2} - m_{S2}}\right) \times \left(\frac{\kappa_3 \sinh{\tfrac{1}{2}}\kappa_3 \cosh{\tfrac{1}{2}}\kappa_3}{\kappa_2 \sinh{\tfrac{1}{2}}\kappa_2 \cosh{\tfrac{1}{2}}\kappa_2}\right). \quad \text{(C2)}$$

Another equation relating b_1 and a_2 may be obtained from (22), which reduces to

$$a_2^2 = \left[\kappa_2 \sinh{\tfrac{1}{2}}\kappa_2 \cosh{\tfrac{1}{2}}\kappa_2 \left(\frac{m_{A2} - m_{S2}}{m_{A2} - \lambda_2}\right)\left(\frac{\lambda_3 - \lambda_2}{\lambda_3 - \lambda_1}\right)\right]^{-1} \times \left\{\mathcal{E}(0) - \left[\frac{m_{A1} - m_{S1}}{\lambda_1 - m_{S1}} \kappa_1 \sinh{\tfrac{1}{2}}\kappa_1 \cosh{\tfrac{1}{2}}\kappa_1\right] b_1^2\right\}. \quad \text{(C3)}$$

Introduction of (C3) into (C1), followed by integration, yields

$$b_1 = -\left[\frac{\mathcal{E}(0)}{\left(\frac{m_{A1} - m_{S1}}{\lambda_1 - m_{S1}}\right)\kappa_1 \sinh{\tfrac{1}{2}}\kappa_1 \cosh{\tfrac{1}{2}}\kappa_1}\right]^{1/2} \tanh\left\{\left[\left(\frac{m_{A2} - m_{S2}}{m_{A2} - \lambda_2}\right)\left(\frac{\lambda_3 - \lambda_2}{\lambda_3 - \lambda_1}\right)\kappa_2 \sinh{\tfrac{1}{2}}\kappa_2 \cosh{\tfrac{1}{2}}\kappa_2\right]^{-1} \times \left(\frac{\Gamma}{\beta\kappa_1 \cosh{\tfrac{1}{2}}\kappa_1}\right)\left[\mathcal{E}(0)\kappa_1 \sinh{\tfrac{1}{2}}\kappa_1 \cosh{\tfrac{1}{2}}\kappa_1 \left(\frac{m_{A1} - m_{S1}}{\lambda_1 - m_{S1}}\right)\right]^{1/2}\left[\cosh{\tfrac{1}{2}}\kappa_2 \sinh{\tfrac{1}{2}}\kappa_3 (m_{A3} - m_{S2})\left(\frac{\lambda_3 - m_{S3}}{m_{A2} - \lambda_2}\right)^{1/2} + \sinh{\tfrac{1}{2}}\kappa_2 \cosh{\tfrac{1}{2}}\kappa_3 (m_{S3} - m_{A2})\left(\frac{m_{A3} - \lambda_3}{m_{A2} - \lambda_2}\frac{\lambda_2 - m_{S2}}{m_{A2} - \lambda_2}\right)^{1/2}\right](t_0 - t)\right\}, \quad \text{(C4)}$$

where the integration constant has been determined by setting $t = t_0$ when $b_1 = 0$. The amplitude a_2 may then be determined and expressed as

$$a_2 = \left[\frac{\mathcal{E}(0)}{\left(\frac{m_{A2} - m_{S2}}{m_{A2} - \lambda_2}\right)\left(\frac{\lambda_3 - \lambda_2}{\lambda_3 - \lambda_1}\right)\kappa_2 \sinh{\tfrac{1}{2}}\kappa_2 \cosh{\tfrac{1}{2}}\kappa_2}\right]^{1/2} \operatorname{sech}\left\{\left[\left(\frac{m_{A2} - m_{S2}}{m_{A2} - \lambda_2}\right)\left(\frac{\lambda_3 - \lambda_2}{\lambda_3 - \lambda_1}\right)\kappa_2 \sinh{\tfrac{1}{2}}\kappa_2 \cosh{\tfrac{1}{2}}\kappa_2\right]^{-1} \times \left(\frac{\Gamma}{\beta\kappa_1 \cosh{\tfrac{1}{2}}\kappa_1}\right)\left[\mathcal{E}(0)\kappa_1 \sinh{\tfrac{1}{2}}\kappa_1 \cosh{\tfrac{1}{2}}\kappa_1 \left(\frac{m_{A1} - m_{S1}}{\lambda_1 - m_{S1}}\right)\right]^{1/2}\left[\cosh{\tfrac{1}{2}}\kappa_2 \sinh{\tfrac{1}{2}}\kappa_3 (m_{A3} - m_{S2})\left(\frac{\lambda_3 - m_{S3}}{m_{A2} - \lambda_2}\right)^{1/2} + \sinh{\tfrac{1}{2}}\kappa_2 \cosh{\tfrac{1}{2}}\kappa_3 (m_{S3} - m_{A2})\left(\frac{m_{A3} - \lambda_3}{m_{A2} - \lambda_2}\frac{\lambda_2 - m_{S2}}{m_{A2} - \lambda_2}\right)^{1/2}\right](t_0 - t)\right\}. \quad \text{(C5)}$$

The relationship obtained between the amplitudes shows that a_1 is proportional to the hyperbolic tangent and the remaining amplitudes are proportional to the hyperbolic secant. Finally, introduction of (33) and (34) into (C4) and (C5) provides the form of the solutions given by (38) and (39).

REFERENCES

Blumen, W., 1978a: Uniform potential vorticity flow: Part I. Theory of wave interactions and two-dimensional turbulence. *J. Atmos. Sci.*, **35**, 774–783.

——, 1978b: Uniform potential vorticity flow: Part II. A model of wave interactions. *J. Atmos. Sci.*, **35**, 784–789.

Charney, J. G., 1971: Geostrophic turbulence. *J. Atmos. Sci.*, **28**, 1087–1095.

Fjørtoft, R., 1953: On the changes in the spectral distribution of kinetic energy for two-dimensional non-divergent flow. *Tellus*, **5**, 225–230.

Morse, P. M., and K. U. Ingard, 1968: *Theoretical Acoustics.* McGraw-Hill, 927 pp.

Pedlosky, J., 1964: The stability of currents in the atmosphere and oceans: Part I. *J. Atmos. Sci.*, **21**, 201–219.